Dimerized ground state and magnetic excitations in $CaCuGe_2O_6$

A. Zheludev and G. Shirane
Brookhaven National Laboratory, Upton, New York 11973-5000

Y. Sasago, M. Hase,* and K. Uchinokura
Department of Applied Physics, The University of Tokyo, Bunkyo-ku, Tokyo 113, Japan
(Received 20 November 1995)

The $S=\frac{1}{2}$ Heisenberg antiferromagnet $CaCuGe_2O_6$ was studied by inelastic neutron scattering on a powder sample in the temperature range 5–300 K. A sharp symmetric magnetic inelastic peak was observed around $\hbar\omega=6$ meV, and its q and temperature dependences were investigated. The absolute values of the energy-integrated magnetic intensity were determined. Despite the fact that from the structural point of view the material has a distinct one-dimensional arrangement of magnetic sites, the experimental results are surprisingly well described by an ensemble of weakly interacting antiferromagnetic dimers, which are composed of pairs of Cu^{2+} ions.

I. INTRODUCTION

In recent years much attention has been given to magnetic systems which, for various reasons, have a ground state with no long-range order in the two-spin correlation function and an energy gap in the magnetic excitation spectrum. These properties may result from quantum spin fluctuations in low-dimensional structures, as in Haldane-gap integer-S systems (Refs. 1,2, and references therein). Alternatively, the dimerized spin-singlet ground state in spin-Peierls materials is stabilized by a modulation of the crystal lattice.[3–7] Several other systems with a gap and a nonmagnetic ground state, for example, spin ''ladders,'' have also been studied (see, for example, Refs. 8–10).

Recently Sasago *et al.*[11] discovered a singlet ground state in $CaCuGe_2O_6$, a material related to spin-Peierls $CuGeO_3$. $CaCuGe_2O_6$ has a strongly distorted pyroxene-type structure, typical of many germanates and silicates.[12] The lattice is monoclinic (space group $P2_1/c$), the room-temperature cell constants being $a=10.198$ Å, $b=9.209$ Å, $c=5.213$ Å, and $\beta=105.73°$.[13] The magnetism of this material is due to $S=\frac{1}{2}$ Cu^{2+} ions, which are arranged in zigzag chains along the c direction. Intrachain Cu-Cu distances are 3.072 Å. dc magnetic susceptibility measurements clearly indicate an exponential behavior of $\chi(T)$ at $T\rightarrow 0$ (Fig. 1, inset). Despite the obvious linear-chain structural arrangement of the magnetic ions in the crystal, the magnetization and susceptibility data are inconsistent with theoretical expectations for a quasi-one-dimensional (quasi-1D) spin system. The model proposed by Sasago *et al.* is based on the idea that particular pairs of magnetic ions tend to form weakly interacting antiferromagnetic (AF) dimers. In fact, $\chi(T)$ may be well fit by the susceptibility of noninteracting dimers with a singlet-triplet energy gap $\Delta\approx 68$ K$=5.9$ meV (dotted line in the inset in Fig. 1). Similar properties have been previously found in organometallic molecular compounds.[14] $CaCuGe_2O_6$ is the first example of an ionic structure, with densely packed magnetic ions, in which this type of behavior is observed. Bulk magnetic measurements by Sasago *et al.* indeed provide valuable information on the system, proving the existence of a dimerized state. However, to unambiguously determine which particular pairs of Cu ions actually contribute to the dimerization process and what the intradimer spin separation is, one has to exploit space-resolving methods, such as neutron scattering.

This paper deals with an inelastic neutron scattering in-

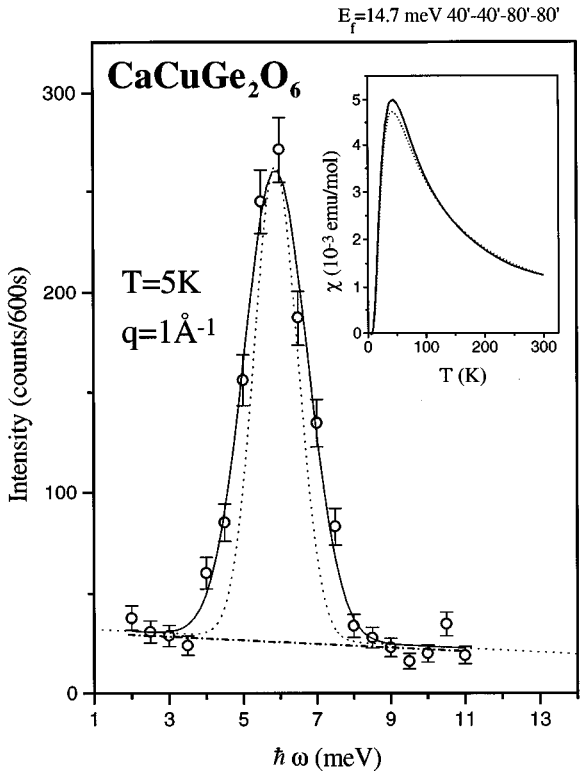

FIG. 1. Constant-q scan measured in $CaCuGe_2O_6$ powder sample at $T=5$ K and $q=1$ Å^{-1}. The solid line is a Gaussian fit, and the dashed line represents the experimental resolution function. Inset: magnetic susceptibility of $CaCuGe_2O_6$ (solid line) and that of an isolated antiferromagnetic dimer (dashed line).

vestigation of a $CaCuGe_2O_6$ powder sample. Our main result is the observation of a well-defined symmetric inelastic magnetic peak at $\hbar\omega \approx 6$ meV. Its intensity is found to be strongly temperature and q dependent. The results confirm the existence of a dimerized ground state and provide an estimate for the intradimer spin-spin distance.

II. NEUTRON SCATTERING EXPERIMENTS

The preparation of $CaCuGe_2O_6$ powder samples is described in Ref. 11. Only a small amount of material, ≈ 1.8 g, was available for the neutron scattering experiments. The measurements were performed at the High Flux Beam Reactor at Brookhaven National Laboratory. We have first measured a neutron powder diffraction profile, which was found to be completely consistent with the crystal structure reported in Ref. 13. The inelastic measurements were performed at the H7 and H8 triple-axis spectrometers, using PG (pyrolitic graphite) (002) reflections for monochromator and analyzer. Several spectrometer configurations were exploited. Most of the data were collected using a fixed final neutron energy $E_f = 14.7$ meV, a 40′-40′-80′-80′ collimation, and a PG filter positioned after the sample to eliminate higher-order beam contamination. This setup yields an energy resolution of $2\Gamma = 0.97$ meV at $q = 1$ Å^{-1} and $\hbar\omega = 0$, as determined from measuring the incoherent scattering from the sample. The use of a configuration with a fixed incident neutron energy $E_i = 14.7$ meV and a PG filter in front of the sample provided a better signal-to-noise ratio, but effectively limited the accessible energy-loss range to 8 meV at $q = 1$ Å^{-1}, the analyzer efficiency being strongly reduced at higher-energy transfers. The sample was mounted in a Displex refrigerator which allowed us to perform the measurements over a wide temperature range 5–300 K.

A constant-q inelastic scan taken at $q = 1$ Å^{-1}, $T = 5$ K is shown in Fig. 1. The dotted line represents the energy resolution profile calculated for $\Delta E = 6$ meV. A well-defined *symmetric* inelastic peak is observed at $\hbar\omega = 5.9$ meV. No other features were observed for energy transfers up to 20 meV. The peak position is practically temperature independent, but the intensity decreases rapidly with increasing temperature (Fig. 2). Above $T \approx 100$ K the intensity levels off and the peak is still well observed at 300 K. The background intensity, measured at $\hbar\omega = 3$ meV and 9 meV, remains constant over the entire temperature range 5–300 K. Even at 5 K the inelastic peak has a finite total energy width of $2\Gamma = 2.0$ meV full width at half maximum (FWHM), as measured using the 40′-40′-80′-80′, $E_f = 14.7$ meV setup. Note that this width is larger than the experimental resolution, which at $\hbar\omega = 6$ meV was calculated to be $2\Gamma = 1.2$ meV FWHM. Only a relatively small broadening is observed at higher temperatures (total $2\Gamma \approx 2.8$ meV at 300 K). The energy-integrated intensity of the 6 meV peak measured at $q = 1$ Å^{-1} is plotted against temperature in Fig. 3 (open squares), showing a saturation below 10 K. Above $T \approx 100$ K the curve levels off. Once the temperature dependence of the peak width was established by performing energy scans at several temperatures, the data for Fig. 3 could be collected more rapidly by measuring the peak intensities (at 6 meV) and scaling them to compensate for the changing peak width (solid circles). The q dependence of the inelastic intensity

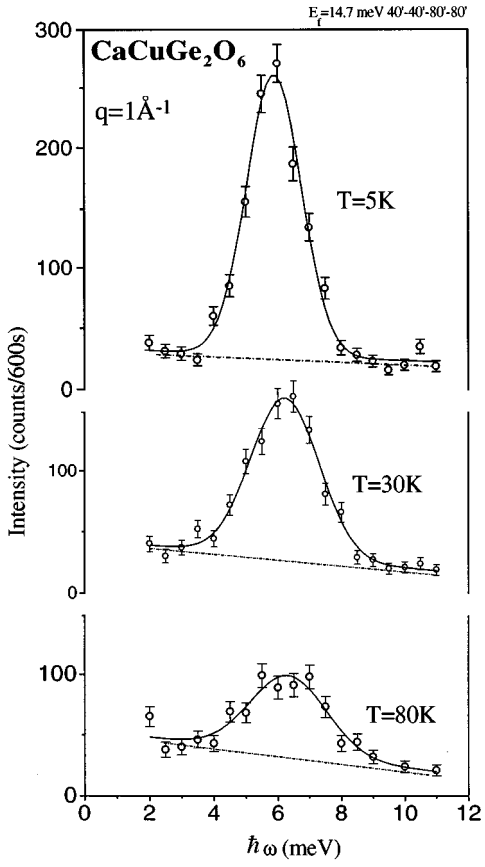

FIG. 2. Temperature dependence of the inelastic peak in $CaCuGe_2O_6$ at $q = 1$ Å^{-1}. The solid lines are Gaussian fits to the data.

measured at $\hbar\omega = 6$ meV is presented in the inset in Fig. 4. The constant-E scan shows a broad symmetric maximum at $q \approx 1$ Å^{-1} and a weaker feature at $q \approx 2$ Å^{-1}. The energy at which the inelastic peak is observed in constant-q scans (6 meV) is q independent in the range 0.7–3 Å^{-1}. This was verified by performing energy scans at $T = 10$ K and $q = 0.7$, 1, 1.1, 1.5, 2, 2.5, and 3 Å^{-1}.

III. ANTIFERROMAGNETIC DIMER MODEL

In all of the 1D systems with a spin gap mentioned in the Introduction, the magnetic excitations have a wide band and a strong dispersion along the chain direction. In result the line shapes in constant E and constant q are to a large extent determined by the shape of the dispersion manifold. In particular, constant-E scans performed at exactly the gap energy show an abrupt cutoff at small q.[16] Constant-q scans through the gap show an extended tail on the high-energy part.[17,16] This type of behavior is clearly inconsistent with our results for $CaCuGe_2O_6$: No cutoff has been observed at the gap energy down to $q = 0.7$ Å^{-1} and the line shapes in constant-q scans are completely symmetric. Although the crystal structure reveals a distinct 1D arrangement of Cu^{2+} ions, there is no strong one-dimensionality in the magnetic excitations. Rather, as suggested by dc susceptibility measurements,[11] at least empirically, the starting point for

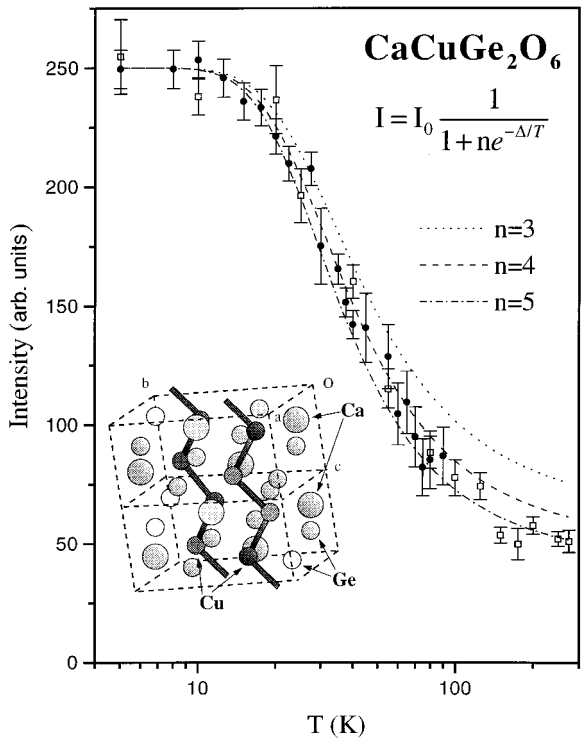

FIG. 3. Temperature dependence of the 6-meV energy-integrated (open squares) and peak intensities (solid circles). The latter are renormalized to account for the temperature-dependent peak width. The background signal has been subtracted. Inset: a schematic representation of the crystal structure of $CaCuGe_2O_6$.

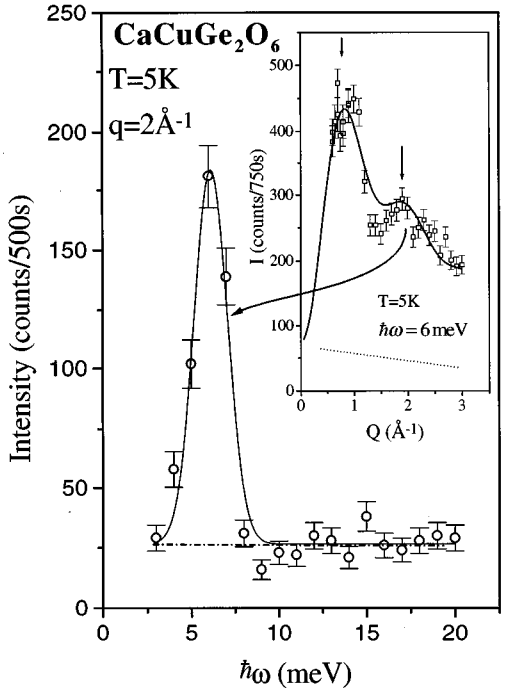

FIG. 4. Constant-q scan measured in $CaCuGe_2O_6$ powder sample at $T=5$ K and $q=2$ Å^{-1}. Inset: q dependence of the inelastic intensity measured at $\hbar\omega=6$ meV. The dashed line shows the background, measured at $\hbar\omega=3$ meV. The solid line represents a fit with Eq. (6).

the interpretation of our experimental data should be a description based on *noninteracting* antiferromagnetic dimers.

A. Cross section

The inelastic cross section for isolated AF dimers was obtained by Furrer and Güdel.[14] For convenience we briefly derive this form here, introducing some new notations and definitions. An isolated system of two $S=\frac{1}{2}$ spins with isotropic AF interaction $\hat{H}=J\hat{\mathbf{S}}_1\hat{\mathbf{S}}_2$ has a nondegenerate ground state with $S=0$,

$$|A\rangle=\frac{1}{\sqrt{2}}\{|\uparrow\downarrow\rangle-|\downarrow\uparrow\rangle\}, \tag{1}$$

and a triplet excited state with $S=1$,

$$\begin{aligned} S_z=0:\quad |B\rangle&=\frac{1}{\sqrt{2}}\{|\uparrow\downarrow\rangle+|\downarrow\uparrow\rangle\};\\ S_z=1:\quad |C\rangle&=|\uparrow\uparrow\rangle;\\ S_z=-1:\quad |D\rangle&=|\downarrow\downarrow\rangle. \end{aligned} \tag{2}$$

The inelastic scattering cross section for unpolarized neutrons is given by[18]

$$\frac{d^2\sigma}{d\Omega\, dE'}=r_0^2\frac{k'}{k}S(\mathbf{q},\omega),$$

$$S(\mathbf{q},\omega)=\sum_{\lambda\lambda'}p_\lambda\langle\lambda|\hat{\mathbf{Q}}_\perp^+(\mathbf{q})|\lambda'\rangle\langle\lambda'|\hat{\mathbf{Q}}_\perp(\mathbf{q})|\lambda'\rangle \times\delta(\hbar\omega+E_\lambda-E_{\lambda'}). \tag{3}$$

Here k and k' are the incident and scattered neutron wave numbers and $r_0=-0.54\times10^{-12}$ cm. The sums are taken over initial and final stationary states of the scattering system λ and λ' with energies E_λ and $E_{\lambda'}$, respectively; p_λ is the thermal population factor for the initial state, and $\hat{\mathbf{Q}}(\mathbf{q})$ is the operator form for the magnetic structure factor of the individual dimer:

$$\hat{\mathbf{Q}}(\mathbf{q})=f(q)[\exp(i\mathbf{q}\cdot\mathbf{d})\hat{\mathbf{S}}^{(2)}+\exp(-i\mathbf{q}\cdot\mathbf{d})\hat{\mathbf{S}}^{(1)}], \tag{4}$$

where $2d$ is the intradimer spin separation, and $f(q)$ is the atomic magnetic form factor. The subscript $\perp$ in Eq. (3) indicates a projection onto a plane perpendicular to the scattering vector. The evaluation of matrix elements in Eq. (3) is straightforward and leads to the following form for the energy-loss part of $S(\mathbf{q},\omega)$ at $T=0$:

$$S(\mathbf{q},\omega)=S_{A\to C}+S_{A\to D}+S_{A\to B}, \tag{5}$$

$$S_{A\to C}=S_{A\to D}=\frac{1}{2}S_{A\to B}=\frac{1}{2}\sin^2(\mathbf{q}\cdot\mathbf{d})|f(q)|^2.$$

To obtain the intensity measured in a powder experiment one has to perform a spherical average of the scattering law (5) over the relative orientation of $\mathbf{q}$ and $\mathbf{d}$. This procedure yields the final expression

$$\frac{d^2\sigma}{d\Omega\, dE'} = r_0^2 \frac{k'}{k} N |f(q)|^2 \left[1 - \frac{1}{2qd} \sin(2qd) \right] \delta(\hbar\omega - \Delta). \tag{6}$$

In this formula $\Delta = J$ stands for the singlet-triplet energy gap, and N is the number of dimers in the sample. Note that the cross section is a maximum at $q = 1.503 \times \pi/(2d)$. At this wave vector the energy-integrated intensity is somewhat larger than that for an ideal paramagnet (at $\hbar\omega = 0$) with $2N$ uncorrelated $S = 1/2$ spins:

$$I_{\max} \approx 1.21 I_{\text{para}}. \tag{7}$$

B. Temperature dependence

At $T \neq 0$ the energy-loss cross section for a two-level system is scaled by the thermal population factor for the ground state:[15]

$$\frac{d^2\sigma}{d\Omega\, dE'}(T) = \frac{1}{1 + n e^{-\Delta/k_B T}} \frac{d^2\sigma}{d\Omega\, dE'}(0). \tag{8}$$

Here n is the degeneracy of the excited state ($n = 3$ for an AF dimer), and k_B is Boltzmann's constant. The dashed lines on Fig. 3 show the temperature dependence that follows from this equation for different values of n and for $\Delta = 6$ meV. We see that the curve for $n = 3$ (the case of noninteracting dimers) fits the data well. This simple model is therefore a good first approximation, although the observed reduction of intensity at high temperatures is somewhat greater than for an $n = 3$ two-level system, and the $n = 4$ and $n = 5$ curves apparently fit the data better. It is important to note that the value for the singlet-triplet energy gap, obtained by Sasago *et al.*[11] by fitting the noninteracted dimer model to the magnetic susceptibility data, is in excellent agreement with that determined by neutron scattering. On the other hand, the gap value deduced from high-field measurements is some 20% *smaller*. This discrepancy may be explained by allowing for weak interdimer interactions, which affect the high-field measurements.[11] Interdimer coupling may also account for the presence of a small dispersion in the 6 meV excitation and the consequent finite intrinsic peak width, observed in this work.

C. Q dependence

Not only does the isolated-dimer model account surprisingly well for the T dependence of the intensity, but can also qualitatively explain the observed q dependence. Since the excitations in this model are dispersionless, the profiles measured in constant-E scans are entirely determined by the structure factor of an isolated dimer. The solid line in Fig. 4 (inset) shows a fit of Eq. (6) to our data. The only adjustable parameters were the overall scaling factor and the dimer size $2d$. We have utilized the Freman-Watson form factor for Cu^{2+}.[19,20] Apart from the fact that the measured q dependence seems to fall off more rapidly at large q than the theoretical curve, the experimental results are qualitatively reproduced. The fitting procedure yielded $2d = 5.4$ Å. This value roughly coincides with the third-nearest-neighbor (3NN) Cu-Cu distance in the crystal (5.55 Å). The measured structure factor is therefore consistent with the models proposed Sasago *et al.*, in which the dimerization occurs between 3NN or 4NN Cu^{2+} ions from adjacent chains. However, we point out that $2d = 5.4$ Å is also close to the 2NN distance between the Cu sites within the zigzag chains (5.21 Å). This ambiguity will be resolved once a single-crystal sample sufficiently large for inelastic neutron scattering experiments becomes available, thanks to the scalar product in Eq. (5), which allows us to determine the orientation of the dimers.

IV. ABSOLUTE INTENSITIES

As described in detail in Ref. 21, energy-integrated magnetic intensities measured on powder samples may be put on an absolute scale by comparing them to intensities of Bragg powder lines. For an ideal paramagnet these intensities are related by the following formula:[21]

$$I_{\text{para}} = M^2 I_{\text{Bragg}}/C, \tag{9}$$

$$C = \frac{1}{0.0485 |f(q)|^2} \frac{1}{8\pi} \frac{\lambda^3 P |F|^2}{N_M V_c \sin\theta \sin(2\theta)},$$

where F and P are the structure factor and multiplicity for the powder reflection, N_M is the number of magnetic atoms per unit cell, V_c is the unit cell volume, and M is the effective moment of the spin carriers. The Bragg intensity I_{Bragg} is the conventional 2θ-integrated powder line intensity (2θ is taken in radians) multiplied by FWHM energy resolution (measured by scanning through the incoherent scattering). For an isolated dimer at $T \ll \Delta$ at the wave vector where the inelastic intensity is a maximum, combining Eq. (7) and Eq. (9) we obtain

$$I_{\max} = 1.21 M^2 I_{\text{Bragg}}/C. \tag{10}$$

In application to $CaCuGe_2O_6$ the (2 0 0) powder line was used. The measurements were performed using 40′-40′-80′-80′ collimation with $\lambda = 2.35$ Å. In our case $F_{(2\,0\,0)} = 2.51 \times 10^{-12}$ cm, $2\theta = 27.8°$, $N_M = 4$, $V_c = 471$ Å^3, $P_{(200)} = 2$, and $2\Gamma = 1.4$ meV, and so $C = 0.64$. Experimentally $I_{\text{Bragg}} = 0.00612$ counts meV/monitor. Using $g = 2$ for Cu, we obtain the estimate $I_{\max}^{(\text{calc})} = 0.035$ counts meV/monitor.

The actual energy-integrated magnetic intensity for $CaCuGe_2O_6$ was measured at $T = 10$ K for $q = q_0 = 1$ Å^{-1}. At this wave vector, assuming $2d = 5.4$ Å, the intensity for the isolated-dimer model is given by $I_{q_0} \approx 0.95 I_{\max}$. From this consideration we obtain the value $I_{\max}^{(\text{expt})} = 0.030$ counts meV/monitor. This is in good agreement with $I_{\max}^{(\text{calc})} = 0.035$ counts meV/monitor. We see that the isolated-dimer model is consistent with our experiments on $CaCuGe_2O_6$ in what concerns the absolute intensities as well. This implies that all the Cu^{2+} ions in the crystal participate in the dimerization process.

V. CONCLUDING REMARKS

Our experiments provide an unambiguous proof that the magnetic excitations in $CaCuGe_2O_6$ may be adequately described by a simple model, in which the system is treated as an array of weakly interacting AF dimers. This type of non-

magnetic ground state has been observed in an ionic crystal with densely packed magnetic ions (as opposed to molecular crystals, in which the dimers are confined in organometallic complexes and are spatially separated). As mentioned above, the surprising fact is that the dimers appear in a material with a pronounced 1D arrangement of magnetic ions. It is well known that a dimerized ground state may occur in AF linear chains with competing interactions[22–27] or even in 3D spin networks.[27] However, the excitation spectrum of such systems is a continuum with a lower threshold and a pronounced dispersion in the latter, at least in the 1D case.[24] This is inconsistent with the behavior observed in $CaCuGe_2O_6$. To explain the properties of this compound one has to look for true, i.e., geometrically distinct, pairs of magnetic ions. Since the Cu chains are uniform, the dimerization cannot occur within the chains, unless the translational symmetry is broken. Such a structural phase transition would manifest itself in the apparition of new superstructure peaks in the diffraction pattern. No superstructure reflections were observed in our experiments, but more precise measurements are required, since such features may in practice be extremely weak, as in the case $CuGeO_3$.[6] One more time we would like to stress that a single-crystal inelastic neutron scattering experiment is highly desirable. In addition to the spin-spin separation $2d$, determined in our powder experiments, single-crystal measurements can be used to identify the vector **d** itself and accurately measure the dispersion of the magnetic excitations. This would immediately resolve the ambiguity which exists due to similar 2NN and 3NN Cu-Cu distances and greatly improve our understanding of the physics underlying the dimerization process.

ACKNOWLEDGMENTS

We would like to thank G. Castilla, V. J. Emery, K. Hirota, and T. Oguchi for illuminating discussions. This study was supported in part by the U.S.-Japan Cooperative Program on Neutron Scattering and NEDO (New Energy and Industrial Technology Development Organization) International Joint Research Grant. Work at Brookhaven National Laboratory was carried out under Contract No. DE-AC02-76CH00016, Division of Material Science, U.S. Department of Energy.

*Present address: The Institute of Physical and Chemical Research (RIKEN), Wako 351-01, Japan.

[1] F. D. M. Haldane, Phys. Rev. Lett. **50**, 1153 (1983).
[2] L. P. Regnault, I. Zaliznyak, J. P. Renard, and C. Vettier, Phys. Rev. B **50**, 9174 (1994).
[3] M. Hase, I. Terasaki, and K. Uchinokura, Phys. Rev. Lett. **70**, 3651 (1993).
[4] M. Hase *et al.*, Phys. Rev. B **48**, 9616 (1993).
[5] H. Kuroe *et al.*, J. Phys. Soc. Jpn. **63**, 365 (1994).
[6] J. P. Pouget *et al.*, Phys. Rev. Lett. **72**, 4037 (1994).
[7] K. Hirota *et al.*, Phys. Rev. Lett. **73**, 736 (1994).
[8] T. M. Rice, S. Gopalan, and M. Sigrist, Europhys. Lett. **23**, 445 (1993).
[9] T. Barnes and J. Riera, Phys. Rev. B **50**, 6817 (1994).
[10] M. Azuma *et al.*, Phys. Rev. Lett. **73**, 3463 (1994).
[11] Y. Sasago *et al.*, Phys. Rev. B **52**, 3533 (1995).
[12] *Pyroxenes*, Vol. 7 of *Reviews in Mineralogy*, edited by C. T. Prewitt (Mineralogical Society of America, 1980).
[13] M. Behruzi, K.-H. Breuer, and W. Eysel, Z. Kristallogr. **176**, 205 (1986).
[14] A. Furrer and H. U. Güdel, Phys. Rev. Lett. **39**, 657 (1977).
[15] R. E. Watson and A. J. Freeman, Acta Crystallogr. **14**, 27 (1961).
[16] J. F. DiTusa *et al.*, Physica B **194** (1994).
[17] J. Darriet and L. P. Regnault, Solid State Commun. **86**, 409 (1993).
[18] S. W. Lovesey, *Theory of Neutron Scattering from Condensed Matter* (Clarendon Press, Oxford, 1984), Vol. 2.
[19] T. Freltoft, G. Shirane, S. Mitsuda, J. P. Remeika, and A. S. Cooper, Phys. Rev. B **37**, 137 (1988).
[20] J. Akimitsu and Y. Ito, J. Phys. Soc. Jpn. **40**, 1621 (1976).
[21] A. I. Goldman *et al.*, Phys. Rev. B **33**, 1627 (1986).
[22] C. K. Majumdar and D. K. Ghosh, J. Math. Phys. **10**, 1388 (1969).
[23] C. K. Majumdar, J. Phys. C **3**, 911 (1970).
[24] B. S. Shastry and D. Sutherland, Phys. Rev. Lett. **47**, 964 (1981).
[25] F. D. Haldane, Phys. Rev. B **25**, 4925 (1982).
[26] T. Tonegawa and I. Harada, J. Phys. Soc. Jpn. **56**, 2153 (1987).
[27] T. Oguchi and H. Kitatani, J. Phys. Soc. Jpn. **64**, 612 (1995).